

## Influence of post-annealing on the properties of Ta-doped $\text{In}_2\text{O}_3$ transparent conductive films

XU Lei<sup>1,2</sup>, WANG Rui<sup>1,2\*</sup>, LIU Yong<sup>1</sup>, ZHANG Dan<sup>1</sup> & XIAO Qi<sup>1</sup>

<sup>1</sup> Key Laboratory of Composite Materials, Tianjin Polytechnic University, Tianjin 300160, China;

<sup>2</sup> School of Textiles, Tianjin Polytechnic University, Tianjin 300160, China

Received December 3, 2010; accepted February 17, 2011; published online April 13, 2011

Ta-doped  $\text{In}_2\text{O}_3$  transparent conductive oxide films were deposited on glass substrates using radio-frequency (RF) sputtering at 300°C. The influence of post-annealing on the structural, morphologic, electrical and optical properties of the films was investigated using X-ray diffraction, field emission scanning electron microscopy, Hall measurements and optical transmission spectroscopy. The obtained films were polycrystalline with a cubic structure and were preferentially oriented in the (222) crystallographic direction. The lowest resistivity,  $5.1 \times 10^{-4} \Omega \text{ cm}$ , was obtained in the film annealed at 500°C, which is half of that of the un-annealed film ( $9.9 \times 10^{-4} \Omega \text{ cm}$ ). The average optical transmittance of the films was over 90%. The optical bandgap was found to decrease with increasing annealing temperature.

**transparent conductive films, transparent semiconductors, Hall measurement, optical bandgap, radio-frequency sputtering**

**Citation:** Xu L, Wang R, Liu Y, et al. Influence of post-annealing on the properties of Ta-doped  $\text{In}_2\text{O}_3$  transparent conductive films. Chinese Sci Bull, 2011, 56: 1535–1538, doi: 10.1007/s11434-011-4450-y

Transparent conductive oxide (TCO) films, which include ZnO [1],  $\text{SnO}_2$  [2] and  $\text{In}_2\text{O}_3$  [3], have been widely employed as transparent electrodes for flat panel displays, solar cells and organic light-emitting diodes. This is because of their good optical transmittance, high electrical conductivity, superior substrate adhesion, chemical inertness and compatibility with microelectronic technology [4–10]. Usually, undoped metal oxides exhibit unacceptably high resistivity for TCO applications. Thus, various metals or metal oxides are employed to enhance the film conductivity. It has been widely reported that doping appropriate impurities into metal oxide films can decrease the resistivity by one or two orders of magnitude [11]. The dopant should be chosen through consideration of both the charge and radius of the atom. For  $\text{In}_2\text{O}_3$ , Ta is a promising dopant, because the radius of  $\text{Ta}^{5+}$  is similar to but smaller than that of  $\text{In}^{3+}$ . Moreover, only small  $\text{In}_2\text{O}_3$  lattice deformations are caused

even if high concentrations of Ta are introduced. Some reports on Ta-doped  $\text{In}_2\text{O}_3$  films exist, but they do not focus on the post-treatment of these films [12,13].

TCO film performance critically depends on the microstructure, which in turn depends on the parameter of its deposition and post-treatment [1–3]. Thus, the annealing process may effectively improve the film performance [14,15]. Deposited films have a high density of structural defects and a low stability. The main contribution of post-annealing may come from the improvement of the crystallinity and the chemisorption or desorption of oxygen from the grain boundaries. These effects can significantly enhance the film properties [14,15]. Accordingly, a detailed study of the annealing process, including annealing temperature, time and environment could provide useful information for better understanding of and improving the properties of Ta-doped  $\text{In}_2\text{O}_3$  films.

Radio-frequency (RF) sputtering is a facile and versatile method for the large-scale synthesis of TCO films. It has an

\*Corresponding author (email: wangrui@tjpu.edu.cn)

exceptionally large deposition area, and allows for uniform in film morphology, thickness and compaction. Moreover, it works with an especially diversified range of material compositions [16]. In this paper, we prepare Ta-doped  $\text{In}_2\text{O}_3$  films on glass substrates using RF sputtering at  $300^\circ\text{C}$ , and then post-treat them at various annealing temperatures. Through this process, we explore the effect of post-annealing on TCO film properties and the effects of metal additives on the electric performance. The dependence of the structural, morphologic, electrical and optical properties of the Ta-doped  $\text{In}_2\text{O}_3$  films on this post-annealing was then characterized.

## 1 Experimental

Ta-doped  $\text{In}_2\text{O}_3$  films were deposited on conventional glass substrates (7105) using an RF sputtering system (JZCK-IVB, Shenyang, China) at  $300^\circ\text{C}$ . A commercially available, sintered ceramic 4 wt%  $\text{Ta}_2\text{O}_5$ -doped  $\text{In}_2\text{O}_3$  target of 99.999% purity and 54 mm in diameter was employed as the source material. The target-to-substrate distance was kept at 6 cm. Before sputtering, the vacuum chamber was evacuated to a base pressure of  $1.0 \times 10^{-3}$  Pa. High purity (99.999%) Ar and (99.999%)  $\text{O}_2$  were introduced through separate mass flow controllers. The target was pre-sputtered in an Ar+ $\text{O}_2$  atmosphere for 20 min to remove any impurities on the surface of the target. The deposition power was fixed at 150 W at a frequency of 13.56 MHz. The total pressure during sputtering was maintained at 1.0 Pa, and the Ar/ $\text{O}_2$  ratio was 12:1. The substrate temperature was held at  $300^\circ\text{C}$ . About 20 min after deposition, the glass substrates with Ta-doped  $\text{In}_2\text{O}_3$  films were post-annealed in the temperature range,  $400$ – $600^\circ\text{C}$ , for 30 min in a  $\text{N}_2$  (99.99%).

X-ray diffraction (XRD) analysis was conducted using a Rigaku D/max-2500 X-ray diffractometer with Cu  $\text{K}\alpha$  radiation ( $\lambda=1.5418$  Å, Tokyo, Japan). Field emission scanning electron microscopy (FE-SEM) images were taken on a JEOL JEM-6700F microscope (Tokyo, Japan) equipped with energy dispersive X-ray (EDX) spectroscopy. The film thickness was measured using a step profiler (AMBIOS Technology INC XP-2, Santa Cruz, CA, USA). Hall-effect measurements were performed in the Van der Pauw configuration with indium ohmic electrodes using a Bio-Rad Microscience HL5500 Hall System (Hercules, CA, USA) at room temperature ( $25^\circ\text{C}$ ). The optical transmission measurements were measured using a spectrophotometer (UV-1700, Shimadzu, Kyoto, Japan).

## 2 Results and discussion

Using EDX, we determined that the Ta content in the films is about 5.28 wt%, which is higher than that in the target. The film thickness was measured to be about 300 nm. Fig-

ure 1 shows the XRD patterns for Ta-doped  $\text{In}_2\text{O}_3$  films before and after annealing at different temperatures. All of the diffraction peaks could be indexed to cubic  $\text{In}_2\text{O}_3$  with a lattice constant of  $a=1.011$  nm (JCPDS card no. 06-0416) [3]. No peaks corresponding to  $\text{Ta}_2\text{O}_5$  are observed, which suggests that the tantalum may have been incorporated into the  $\text{In}_2\text{O}_3$  lattice. The radius of  $\text{In}^{3+}$  and  $\text{Ta}^{5+}$  are 0.081 and 0.073 nm, respectively. Thus, the doped tantalum ions can replace the indium atoms in the lattice. Note that the (222) peak becomes more intense and narrower with increasing annealing temperature, which indicates enhancing film quality.

To quantitatively assess the film quality, the full-width at half-maximum (FWHM) values of the (222) peak and the crystallite dimension were estimated according to Scherrer's formula [17],  $t = 0.9\lambda/\beta\cos\theta$ , where  $\lambda$  is the X-ray wavelength,  $\beta$  is the full-width at half-maximum of the (222) diffraction line, and  $\theta$  is the diffraction angle of the XRD spectra (Figure 2). The FWHM values are  $0.261^\circ$ ,  $0.253^\circ$ ,  $0.219^\circ$  and  $0.21^\circ$  for the Ta-doped  $\text{In}_2\text{O}_3$  films before and after annealing at  $400^\circ\text{C}$ ,  $500^\circ\text{C}$  and  $600^\circ\text{C}$ , respectively.

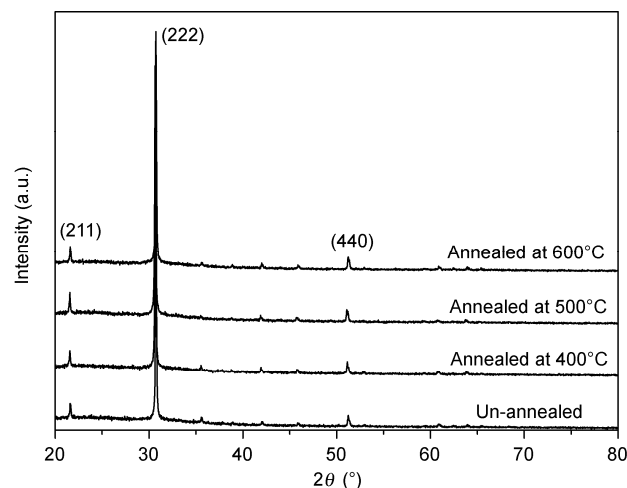


**Figure 1** XRD patterns for the Ta-doped  $\text{In}_2\text{O}_3$  films before and after annealing at different temperatures.

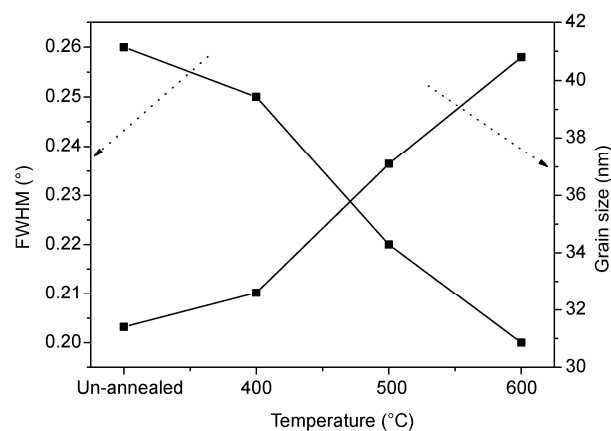
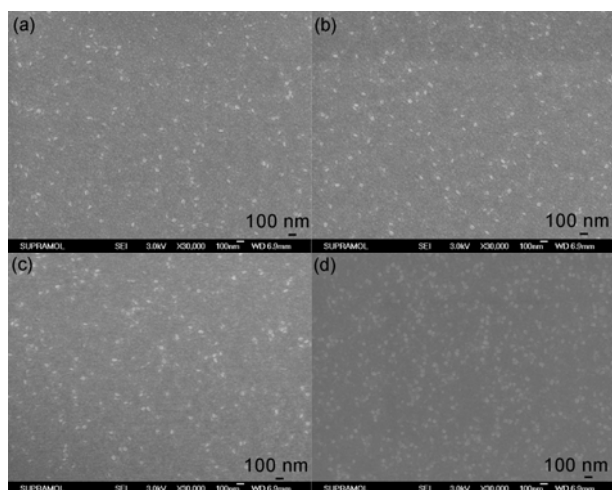


**Figure 2** FWHM of the (222) XRD peak and the grain size of Ta-doped  $\text{In}_2\text{O}_3$  films before and after annealing at various temperatures.

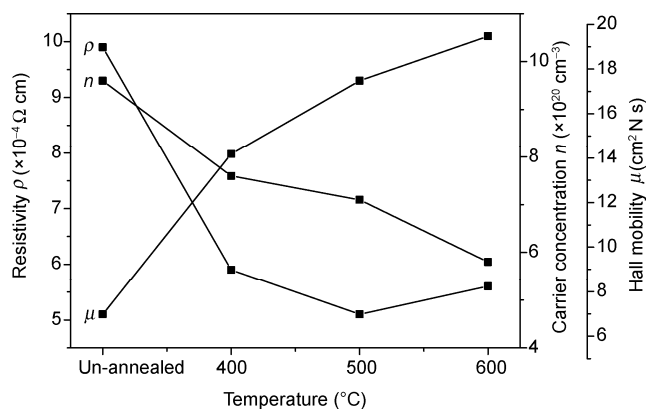
The corresponding crystallite dimensions are about 31.4, 32.6, 37.1 and 40.8 nm, respectively.

Figure 3 shows the surface morphologies of the Ta-doped  $\text{In}_2\text{O}_3$  films before and after annealing at 400°C, 500°C and 600°C. The obtained grains were continuous and dense. The crystallite sizes were found to increase with increasing annealing temperature, which agrees with the XRD results. This is because the ions or ion clusters have more energy at high annealing temperature, which increases their mobility allowing the adjustment of their bond direction and length [18]. This allows the grain size to increase and improve the film crystallinity.

Figure 4 shows the variation in resistivity, carrier concentration and Hall mobility as a function of the annealing temperature for the Ta-doped  $\text{In}_2\text{O}_3$  films. The results showed that all the films were degenerate doped n-type semiconductors. Compared with original film, the annealed films exhibit increased conductivity. The lowest resistivity,  $5.1 \times 10^{-4} \Omega \text{ cm}$ , was measured in the film that was post-annealed at 500°C. This is half of the value of that of the



**Figure 3** SEM images of Ta-doped  $\text{In}_2\text{O}_3$  films before (a) and annealed at 400°C (b), 500°C (c) and 600°C (d).



**Figure 4** Resistivities ( $\rho$ ), carrier concentrations ( $n$ ) and Hall mobility ( $\mu$ ) as a function of annealing temperature for the Ta-doped  $\text{In}_2\text{O}_3$  films.

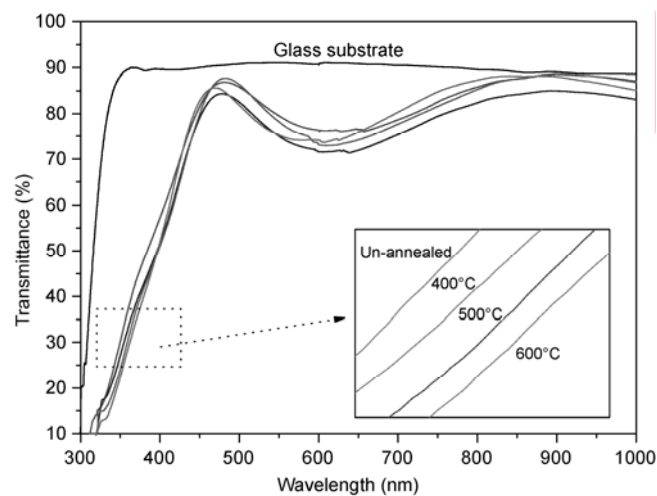
un-annealed film ( $9.9 \times 10^{-4} \Omega \text{ cm}$ ). The effect of post-annealing on film resistivity can be explained by considering both the total change in the carrier concentration and mobility. The mobility increases with increasing annealing temperature. This finding is in accordance with the measured improvement in the film crystallinity [19]. However, the carrier concentration was found to decrease. This is because there was more un-oxidized In in the film, which can be transformed to  $\text{In}_2\text{O}_3$  at high annealing temperatures. Moreover, the corresponding increase in O concentration is favorable for the formation of  $\text{Ta}_2\text{O}_5$ , which contributes to the decrease in carrier concentration [19].

Figure 5 shows the transmittance of the Ta-doped  $\text{In}_2\text{O}_3$  films before and annealing at various temperatures. All of the films have a high optical transmittance with average of 85% over a significant portion of the visible wavelength spectrum (500–800 nm) for the films and the glass substrates. This corresponds to over 90% for the Ta-doped  $\text{In}_2\text{O}_3$  films when 90% average glass substrate transmission is accounted for. As the annealing temperature increases, the absorption edge shifts to longer wavelengths, which is known as the Burstein-Moss shift [20].

The optical bandgap ( $E_g$ ) of the films can be obtained by plotting  $\alpha^2-h\nu$  ( $\alpha$  is the absorption coefficient and  $h\nu$  is the photon energy). Then, we extend plot to the energy axis through extrapolation of its linear component of this plot [11]. The optical bandgaps were 3.91, 3.86, 3.85 and 3.82 eV for Ta-doped  $\text{In}_2\text{O}_3$  films before annealing and after annealing at 400, 500 and 600°C, respectively (Figure 6). The obtained optical bandgaps for these films were larger than that of undoped  $\text{In}_2\text{O}_3$  (3.75 eV) because of the Burstein-Moss effect [20]. The variation in the optical bandgap is closely related to the carrier concentration.

### 3 Conclusions

In conclusion, Ta-doped  $\text{In}_2\text{O}_3$  films were deposited on



**Figure 5** Transmittance spectra of the Ta-doped  $\text{In}_2\text{O}_3$  films before and annealing at various temperatures.

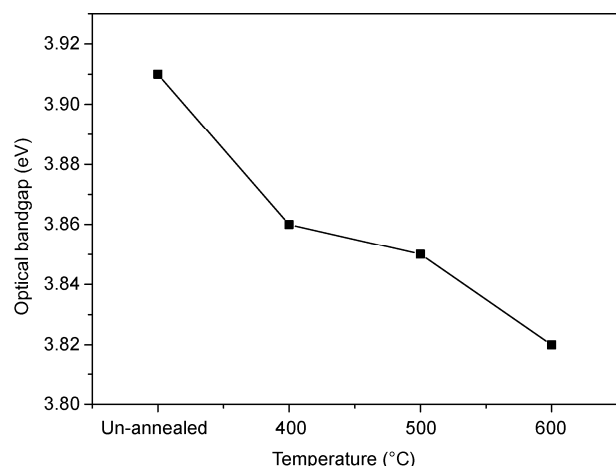


**Figure 6** Optical bandgap of the Ta-doped  $\text{In}_2\text{O}_3$  films before and after annealing at various temperatures.

glass substrates at 300°C by RF sputtering. The effects of post-annealing on the structural, morphologic, electrical and optical properties of the films were investigated. The deposited films were polycrystalline with a bixbyite cubic phase and a preferential orientation of (222) with respect to their substrates. The lowest resistivity,  $5.1 \times 10^{-4} \Omega \text{ cm}$ , was measured in the film post-annealed at 500°C. This is half of the value of that of the un-annealed film ( $9.9 \times 10^{-4} \Omega \text{ cm}$ ). The average optical transmittance of the films was over 90% over the range between 500–800 nm. The optical bandgap was found to decrease with increasing annealing temperature. The results revealed that post-annealing can be used to improve the properties of  $\text{In}_2\text{O}_3$ -based TCO films. We also demonstrated the potential application of Ta-doped  $\text{In}_2\text{O}_3$  films for fabricating high performance TCO films.

*This work was supported by the National Natural Science Foundation of China (51003073/E0303) and Tianjin Natural Science Foundation (08JC-YBJC11400).*

- Kim J H, Ahn B D, Kim C H, et al. Heat generation properties of Ga doped ZnO thin films prepared by rf-magnetron sputtering for transparent heaters. *Thin Solid Films*, 2008, 516: 1330–1333
- Han J B, Zhou H J, Wang Q Q. Conductivity and optical nonlinearity of Sb doped  $\text{SnO}_2$  films. *Mater Lett*, 2006, 60: 252–254

- Kim H, Horwitz J S, Kushto G P, et al. Transparent conducting Zr-doped  $\text{In}_2\text{O}_3$  thin films for organic light-emitting diodes. *Appl Phys Lett*, 2001, 78: 1050–1052
- Liu L, Zhang T, Li S C, et al. Micro-structure sensor based on ZnO microcrystals with contact-controlled ethanol sensing. *Chinese Sci Bull*, 2009, 54: 4371–4375
- Liu X L, Xu H Y, Yu L L, et al. Self-assembly of ZnO nanoparticles and preparation of bulk ZnO porous nanosolids. *Chinese Sci Bull*, 2005, 50: 612–617
- Wang Y Q, Yuan S L, Song Y X. Magnetism in Mn and Co doped ZnO bulk samples. *Chinese Sci Bull*, 2007, 52: 1019–1023
- Sun J, Bai Y Z, Sun J C, et al. Structural and electrical properties of ZnO films on freestanding thick diamond films. *Chinese Sci Bull*, 2008, 53: 2931–2934
- Mao F Y, Deng H, Dai L P, et al. High quality p-type ZnO film growth by a simple method and its properties. *Chinese Sci Bull*, 2008, 53: 2582–2585
- Yi L X, Xu Z, Hou Y B, et al. The ultraviolet and blue luminescence properties of ZnO:Zn thin film. *Chinese Sci Bull*, 2001, 46: 1223–1226
- Wang B G, Shi E W, Zhong W Z, et al. Morphological characteristics of ZnO crystallites under hydrothermal conditions. *Chinese Sci Bull*, 1997, 42: 1041–1046
- Cao F, Wang Y D, Liu D L, et al. Preparation and characterization of transparent conductive Nb-doped ZnO films by radio-frequency sputtering. *Chin Phys Lett*, 2009, 26: 034210/1–3
- Zhang B, Dong X, Xu X, et al. Preparation and characterization of tantalum-doped indium tin oxide films deposited by magnetron sputtering. *Scripta Mater*, 2008, 58: 203–206
- Ju H, Hwang S, Jeong C O, et al. Low-resistivity indium tantalum oxide films by magnetron sputtering. *Appl Phys A*, 2004, 79: 109–111
- Li L, Fang L, Chen X, et al. Effect of annealing treatment on the structural, optical, and electrical properties of Al-doped ZnO thin films. *Rare Metals*, 2007, 26: 247–253
- Chang J F, Lin W C, Hon M H, et al. Effects of post-annealing on the structure and properties of Al-doped zinc oxide films. *Appl Surf Sci*, 2001, 183: 18–25
- Zhang D H, Yang T L, Wang Q P, et al. Electrical and optical properties of Al-doped transparent conducting ZnO films deposited on organic substrate by RF sputtering. *Mater Chem Phys*, 2001, 68: 233–238
- Rani S, Roy S C, Bhatnagar M C. Effect of Fe doping on the gas sensing properties of nano-crystalline  $\text{SnO}_2$  thin films. *Sens Actuatur B Chem*, 2007, 122: 204–210
- Cebulla R, Wendt R, Ellmer K. Al-doped zinc oxide films deposited by simultaneous rf and dc excitation of a magnetron plasma: Relationships between plasma parameters and structural and electrical film properties. *J Appl Phys*, 1998, 83: 1087–1095
- Ko H, Tai W P, Kim K C, et al. Growth of Al-doped ZnO thin films by pulsed DC magnetron sputtering. *J Crystal Growth*, 2005, 277: 352–358
- Burstein E. Anomalous optical absorption limit in InSb. *Phys Rev*, 1954, 93: 632–633

**Open Access** This article is distributed under the terms of the Creative Commons Attribution License which permits any use, distribution, and reproduction in any medium, provided the original author(s) and source are credited.